

**Lattice stability of aluminum-rare earth binary systems: A first-principles approach**Michael C. Gao,<sup>1,\*</sup> Anthony D. Rollett,<sup>1</sup> and Michael Widom<sup>2</sup><sup>1</sup>*Department of Materials Science and Engineering, 5000 Forbes Avenue, Carnegie Mellon University, Pittsburgh, Pennsylvania 15213, USA*<sup>2</sup>*Department of Physics, 5000 Forbes Avenue, Carnegie Mellon University, Pittsburgh, Pennsylvania 15213, USA*  
(Received 20 December 2006; published 31 May 2007)

The thermodynamics of over 330 compounds in 15 Al-RE (RE=rare earth elements) binary systems is studied via first-principles density-functional theory at low-temperature limit. The calculated phase stabilities at  $T=0$  K are in very good agreement with experimentally reported ones for the majority of the systems. For example, we show the  $\text{Al}_2\text{RE}\cdot\text{cF24}$  structure is the most stable compound phase in each binary and it indeed has the highest (congruent) melting point in each system. In some other cases, we obtain results previously unknown experimentally. For example, we suggest that the structure of the observed compound  $\text{AlTm}_2$  is isostructural with  $\text{Co}_2\text{Si}\cdot\text{oP12}$  (prototype  $\text{Co}_2\text{Si}$ , Pearson symbol  $\text{oP12}$ ), we confirm the stability of  $\text{AlEu}\cdot\text{oP20}$  rather than  $\text{AlEu}\cdot\text{oP18}$  by examining the energetics of vacancy substitution, and we predict the unreported Al-Pm phase diagram. Relative accuracy of different potentials and calculational details are addressed. This study predicts that the Al-RE phase diagrams evolve systematically across the entire RE series, interrupted by anomalies at elements Ce and especially Eu and Yb. Trends in lattice stability across the RE series are explained on the basis of interatomic bonding and strain. This study demonstrates that first-principles calculations can be employed to (1) further examine and improve the experimentally established binary-alloy phase diagrams, and (2) provide accurate enthalpy data for stable and hypothetical compounds and structures.

DOI: [10.1103/PhysRevB.75.174120](https://doi.org/10.1103/PhysRevB.75.174120)

PACS number(s): 71.20.Eh, 64.10.+h

**I. INTRODUCTION**

Due to their interpretative and predictive capacities, first-principles (FP) total-energy calculations are widely employed to study alloy lattice stability, interfacial energies, defect structures, etc.<sup>1–18</sup> For example, Wolverton and Ozolins studied the lattice stability of a series of Al alloys using FP total-energy calculations, and they built a FP-based thermodynamic database for Al alloys.<sup>17</sup> An interesting example is the famous compound  $\text{Al}_2\text{Cu}$  ( $\theta'$ ), which is used for precipitate strengthening in Al alloys. It was long believed to be metastable but was surprisingly shown to be the stable phase at low temperatures.  $\theta'$  becomes unstable only at temperatures above 150–200 °C because of the vibrational entropy of competing  $\theta$  phase.<sup>7</sup> Another example is from the work of Mihalkovic and Widom<sup>10</sup> who studied the complete B-Fe-Y-Zr quaternary system using FP calculations. Their study is not only useful in predicting the complete quaternary phase diagram when the experimental phase diagram is not available but also helpful in elucidating the glass formation mechanism in this important glass forming system. Ghosh and Asta<sup>13</sup> calculated the energetics of 69 intermetallic compounds in Al-Ti, Al-Zr, and Al-Hf systematically and found that the formation enthalpies calculated at 0 K agree with calorimetric data, where available, within a few kJ/mol. Adding vibrational free energy into their FP calculations, Arroyave *et al.*<sup>15</sup> confirmed that the  $\text{ZnZr}_2$  and  $\text{Zn}_2\text{Zr}_3$  compounds, which appear stable in Mg-Zn-Zr system, are true equilibrium phases in the Zn-Zr system, although they are still absent from the established equilibrium phase diagrams.

Recently, using a novel strategy that combines critical experiments, calculations of phase diagrams (CALPHAD) modeling, and FP calculations, Gao *et al.*<sup>12</sup> found that the phase relationship between  $\text{Al}_4\text{RE}\cdot\text{tI10}$  and  $\text{Al}_{11}\text{RE}_3\cdot\text{oI28}$  is inappropriately treated for the Al-La, Al-Ce, Al-Pr, and

Al-Nd systems in the established binary alloy phase diagram handbooks. The structure notation in this paper is [prototype or chemical formula].[Pearson symbol]. The prototype is the name of some commonly known isostructural compound, and the Pearson symbol gives point symmetry, translational symmetry, and number of sites per unit cell. They further identified some new phases such as  $\beta\text{Al}_3\text{Ce}\cdot\text{hR12}$ ,  $\text{AlCe}_2\cdot\text{oP12}$ , and  $\beta\text{Al}_3\text{Nd}\cdot\text{hR12}$  in the Al-Ce and Al-Nd systems and assigned the crystal structures based on FP calculations. In light of their results, it is reasonable to ask the following questions: Are there any phases inappropriately treated or any phases missing in the other Al-RE (RE=rare earth elements) binary phase diagrams? Can one use theoretical tools such as FP calculations to examine such possibilities before extensive experiments are performed? These questions motivate our present study of the Al-RE binary systems in the complete RE series.

Another motivation of the present study is to obtain accurate *ab initio* enthalpy data for the complete Al-RE series, including hypothetical compounds, to assist in the development of multicomponent CALPHAD databases and enhance the accuracy when experimental data are not available. This is important because the formation enthalpy data even for stable compounds are rare and are experimentally difficult to measure (e.g., see Table III in this paper). When studying multicomponent ( $\geq 3$ ) system, it is frequently observed that atomic substitution between elements that obey the Hume-Rothery rules is favored in many compounds even if the corresponding edge binary compounds may not be stable. For example, Zanicchi *et al.*<sup>19</sup> studied the phase equilibria of the Al-La-Y ternary system and found that Y atoms substitute for La atoms to form several substitutional solution compounds including  $\text{Al}_{11}(\text{Y}_x\text{La}_{1-x})_3\cdot\text{oI28}$ , even though  $\text{Al}_{11}\text{Y}_3\cdot\text{oI28}$  does not appear in the Al-Y binary equilibrium phase diagram.<sup>20,21</sup> In this scenario, the enthalpy and entropy

of the hypothetical  $\text{Al}_{11}\text{Y}_3$  compound will be needed in a CALPHAD development of the Al-La-Y system. Although these data are very difficult to obtain by experiment since the compound of interest is not stable in the system, it can be obtained from FP calculations and can be directly incorporated into CALPHAD database development.<sup>9,11–13,16</sup>

It is known that for the RE series, both Eu and Yb are divalent in the solid state while all other REs are in the trivalent state. The energy penalty for Eu and Yb to be in the trivalent state is substantial.<sup>22–26</sup> Consequently, systematics are observed for the trivalent RE and their compounds in terms of crystal structures and physical properties (melting point, elastic constants, etc.), whereas anomalies are observed for Eu and Yb.<sup>22,23,27,28</sup> The abnormalities relating to Eu and Yb are probably due to their special electronic configurations. Eu has a half-filled  $4f$  orbital and Yb has completely filled  $4f$  orbital. Both are very stable configurations of low energy, and alloying with Al to form intermetallic compounds disturbs this stable electronic configuration through charge transfer or chemical bonding.

In this paper, we employ FP total-energy calculations to study the thermodynamics of the complete series of Al-RE lanthanide binary systems, aiming to (1) further examine and improve the established Al-RE phase diagrams, (2) examine the reliability of *ab initio* lattice stability in the Al-RE system, (3) provide structural information and thermodynamic properties such as enthalpies of formation for a large set of stable and hypothetical compounds in the Al-RE systems for CALPHAD database development, and (4) physically explain the observed arrangement and anomalies of phase stability in the complete lanthanide RE series in terms of their electronic structures and lattice strain energy.

## II. DETAILS OF FP ENERGY CALCULATIONS

The FP calculations use the plane-wave code VASP,<sup>29,30</sup> which solves for the electronic band structure using electronic density-functional theory (DFT). Because of the presence of RE elements, projector augmented-wave pseudopotentials are used as supplied by VASP. We use the Perdew-Burke-Ernzerhof (PBE) gradient approximation<sup>31</sup> to the exchange-correlation functional. Two choices of potentials are available for each RE element (except La, Tb, Dy, Ho, and Er): a “standard” version in which the entire set of  $f$  levels is treated within the valence band and a divalent or trivalent version (e.g., “Yb\_2” for Yb and “Pm\_3” for Pm) in which some  $f$  electrons are kept frozen in the core. There are several exceptions: (1) there is only a standard potential available for La because it has no occupied  $f$  levels in its elemental state and (2) there is *only* a trivalent version of potential available for Tb, Dy, Ho, and Er with VASP. Although a previous study<sup>18</sup> found that Ce\_3 generates an erroneous energy for  $\text{CeCo}_2$  in Ce-Co, for consistency with other REs, we focus on the Ce\_3 potential in this study. For all other RE elements, the trivalent or divalent potentials are used to gain efficiency in computation and for consistency with cases where the standard potential is not available. Comparisons between the standard and frozen potentials are presented for Ce/Ce\_3, Gd/Gd\_3, and Yb/Yb\_2. The

choice of RE potential with VASP was also discussed in Refs. 12, 18, and 32.

Reciprocal space ( $k$ -point) meshes are increased to achieve convergence to a precision of better than 10 meV/at. with most of the calculations better than 5 meV/at. All structures are fully relaxed (both lattice parameters and atomic coordinates) until energies converge to a precision of 1 meV/at. A “medium precision” setting, which sets the default plane-wave kinetic-energy cutoff, is used for all calculations. The accuracy of “medium precision” was compared with “high precision” for RE elements by Wang *et al.*<sup>9</sup> and also compared for Al-Pm binary compounds.<sup>32</sup> The difference in the enthalpy data of RE elements or Al-Pm compounds due to the choice of precision is negligible, agreeing with our earlier studies on the Al-Ce system.<sup>12</sup> The plane-wave energy cutoff is held constant across each binary system. We choose specific values of the cutoff as 240 eV (the default energy cutoff for Al) for Al-La and Al-Pr, 270 eV (the default energy cutoff for Ni) for Al-Nd since we are currently studying Al-Nd-Ni system, and 293 eV (the default energy cutoff for Fe) for all other binaries since we are interested in extending our study into Al-Fe-RE ternaries in the near future except Al-Ce, in which 300 eV is used for the standard Ce potential for consistency with a study of Al-Ce-Co.

Spin polarization with collinear magnetization is considered in all calculations other than pure aluminum. The magnetic contribution to the total energy is only significant when the standard RE potentials are used; it is essentially zero or negligible if the trivalent or divalent potentials are used, even for elements that are known to be ferromagnetic at room temperature such as Gd. This is because of the fact that, for RE elements, the unpaired  $4f$  electrons are primarily responsible for magnetism, and treating these electrons as frozen core causes loss of magnetism. Although the magnetic structures of pure RE and their binary aluminides are not the focus of this study, the choice of potentials and the corresponding contribution to the total energy due to magnetization on the lattice stability of RE and Al-RE might be important. We explore this using Gd/Yb as a representative test case by calculating pure elemental Gd/Yb using the standard Gd/Yb potential. We also examine the impact of (collinear and noncollinear) electron-spin polarization and electron spin-orbital coupling on both the Gd/Yb and Gd\_3/Yb\_2 potentials. The results listed in Table I show that magnetism and spin-orbital coupling account for a few kJ/mol for Gd, Gd\_3, Yb, and Yb\_2. In most cases, this is too small to alter the assignment of phase stability. However, in some borderline cases, it could be important.

One objective of this study is to predict whether any compounds are missing or improperly treated in the established equilibrium Al-RE binary phase diagrams, e.g., ones that would only be stable at high temperatures such as the  $\text{Al}_3\text{Ce}$  and  $\text{AlCe}_2$  recently identified by Gao *et al.*<sup>12</sup> Therefore, we calculate and then compare the total energy for all “likely” crystal structures for each compound  $\text{Al}_x\text{RE}_y$ . The structure information is primarily taken from Refs. 20, 21, and 33. Reference 33 contains a large body of compound crystal structures, although some might not be stable (i.e., some are metastable, unstable, or wrong). How-

TABLE I. Formation enthalpy of RE elements in several common structures calculated from FP at  $T=0$  K, with respect to their corresponding SER states (in bold). The relative stability is also illustrated in Figs. 1–3.

Lattice	Enthalpy of formation (kJ/mol of atoms)																	
	La	Ce_3 <sup>a</sup>	Pr_3 <sup>b</sup>	Nd_3	Pm_3	Sm_3 <sup>c</sup>	Eu_2	Gd_3 <sup>d</sup>	Gd_3 <sup>e</sup>	Gd <sup>d</sup>	Gd <sup>e</sup>	Tb_3 <sup>f</sup>	Dy_3 <sup>g</sup>	Ho_3	Er_3	Tm_3	Yb_2	Lu_3
Mg.hP2	3.0	1.9	2.8	2.5	2.6	2.9	1.8	<b>0.0</b>	<b>0.0</b>	<b>0.0</b>	<b>0.0</b>	<b>0.0</b>	<b>0.0</b>	<b>0.0</b>	<b>0.0</b>	0.0	0.5 <sup>h</sup>	<b>0.0</b>
La.hP4	<b>0.0</b>	-0.8	<b>0.0</b>	<b>0.0</b>	<b>0.0</b>	0.6	1.7	-1.6	-1.7	4.6	2.7	-1.2	-0.5	3.2	0.7	1.3	0.3	1.9
Sm.hR3	0.3	0.1	2.4	2.3	2.3	<b>0.0</b>	3.1	-1.6	0.6	0.6	2.0	-1.4	-0.8	-0.1	0.1	0.6	0.4	0.7
W.cI2	12.6	10.9	12.2	12.6	13.3	14.2	<b>0.0</b>	12.4	24.4	8.4	8.5	12.7	13.3	13.6	13.8	13.9	0.7 <sup>i</sup>	13.4
Cu.cF4	0.5	<b>0.0</b>	0.9	0.9	1.0	1.5	1.5	-0.6	-0.8	4.8	0.9	0.0	0.9	1.6	2.3	3.1	0.0	4.1

<sup>a</sup>Ce\_3: 2.0 (oC4); -0.2 (tI2). Ce: 8.6 (hP2); 4.4 (hP4); 7.9 (hR3); 22.2 (cI2); 3.47 (U.oC4); and -0.1 (In.tI2). Only collinear electron-spin polarization is considered.

<sup>b</sup>Pr\_3: 0.77 (Pr.hP8); 0.87 (Np.tP4); and 1.16 (Pr.hP6).

<sup>c</sup>Sm\_3: 1.54 (In.tI2).

<sup>d</sup>Only collinear magnetization due to electron-spin polarization is considered.

<sup>e</sup>Considering spin-orbital magnetization coupling and noncollinear magnetism.

<sup>f</sup>Tb\_3: -0.77 (Pr.hP6).

<sup>g</sup>Dy\_3: 0.1 (Dy.oC4).

<sup>h</sup>Yb\_2: 0.5 (hP2); Yb: 0.3 (hP2), when considering spin-orbital magnetization coupling. Yb: 0.4 (hP2) when considering electron-spin polarization only.

<sup>i</sup>Yb\_2: 0.6 (cI2); Yb: 0.0 (cI2), when considering spin-orbital magnetization coupling.

ever, we computed all the reported structures. On the other hand, Ref. 21 sometimes offers more detailed reviews on the phase diagrams, crystal structures, and compositions for all phases; thus, it can be considered as complementary to Ref. 33. Based on the structure information from both sources, we calculate and then compare the total energy for all likely crystal structures for each compound  $Al_xRE_y$ . For instance, we examined five structures for the  $Al_3RE$  compound, including  $AuCu_3.cP4$ ,  $Ni_3Sn.hP8$ ,  $Ni_3Ti.hP16$ ,  $BaPb_3.hR12$ , and  $Al_3Ho.hR20$ , although there may be only one structure stable in an Al-RE binary system. This strategy has been previously applied to predict stable phases in the unreported systems of Al-Pm and Ac-Al (Ref. 32) and B-Fe-Y-Zr.<sup>10</sup>

To obtain enthalpy of formation values  $\Delta H_f$ , a composition-weighted average of the pure elemental cohesive energies is subtracted from the cohesive energy of a given compound. The resulting energy is an “enthalpy” because its volume is relaxed at zero pressure. The phase stability at 0 K is evaluated by a convex hull plot (see Figs. 2 and 3 for example). Vertices of the convex hull of a scatter plot of  $\Delta H_f$  versus composition identify stable structures. Points above the convex hull represent thermodynamically unstable structures at  $T=0$  K, though they may become metastable, or stable at higher temperatures in some cases.

### III. RESULTS

In this section, we present our FP calculation results. We first address the pure elements focusing on the common crystal structures and sequence of thermal stability. Then, we describe the Al-early RE systems whose phase diagrams (except for Al-Eu) appear similar to each other. Then, the Al-late RE systems are addressed as another group. Calculated formation enthalpies of common lattices for pure RE are listed in Table I. Those for a series of stable and hypothetical bi-

nary compounds are listed in Table II. Available values of the formation enthalpies of stable binary compounds measured by various experiments are shown separately in Table III. A summary comparison between FP-predicted lattice stability and experimental observation is shown in Table IV. In order to explain the observed trends in formation enthalpies of compounds and the relative compound stability for the complete RE series, we examine the effect of lanthanide contraction on the lattice strain energy of compounds, focusing on interatomic pair distances.

#### A. Pure elements

For each element, we examine its reported crystal structures and hypothetical ones that, however, are common among REs. Specifically, we compare the prototypes Cu.cF4 (fcc), Mg.hP2 (hcp), La.hP4 (dhcp), W.cI2 (bcc), and Sm.hR3. For example, the low-temperature stable lattice for Sm is Sm.hR3, but the Sm.hR3 prototype is stable only under high pressure for other late REs such as Dy, Lu, and Tm and is not reported at all in other cases. In this study, we calculate the Sm.hR3 lattice stability for all the RE elements for the purpose of comparison. The resulting enthalpies of each element in various crystal structures with respect to the SER state are listed in Table I, which can be directly used as input for CALPHAD database development.<sup>9,11–18</sup> The term “SER” in the CALPHAD community refers to the stable element reference (SER) state, i.e., the stable structure of the pure elements at  $T=298.15$  K and  $P=1.013 \times 10^5$  Pa.

The lattice stability of all 15 RE elements observed in experiments is reasonably reproduced in our FP calculations, except for Gd, Tb, and Dy. In these cases, the FP calculations using RE\_3 potentials predict that both the hR3 and hP4 lattices have a lower energy than the experimentally reported hcp by 0.5–1.6 kJ/mol. This contradicts experiments show-

ing that the Sm.hR3 prototype becomes stable only at high pressure for these elements. Including spin-orbital coupling for Gd does not improve the result (see Table I). We believe that this discrepancy is due to the absence of magnetism. In contrast, calculations using the standard Gd potential considering collinear spin polarization (without spin-orbital coupling) correctly predict that the hcp lattice has the lowest energy at 0 K (see Table I). Further including spin-orbital coupling reveals essentially the same energy within the uncertainty of this calculation (see Table I). Therefore, we conclude that failure to predict the stable lattice of hcp for Gd (and presumably Tb and Dy at 0 K) is due to the choice of trivalent potential. Nevertheless, comparison of both potentials shows that the energies among hR3, hP4, and hcp are very close.

The relative stability of each lattice structure with respect to fcc is illustrated in Fig. 1(a), which shows strong systematics for the majority of the REs but shows anomalies at Eu and Yb. Eu and Yb are special cases because of their half-filled and full-filled  $4f$  orbitals. Current FP calculations correctly predict the structures at low temperatures: early REs except Ce (i.e., La, Pr, Nd, Pm) prefer a dhcp structure, late REs (i.e., Ho, Er, Tm, and Lu) prefer a hcp structure, Ce prefers a fcc structure, Eu prefers a bcc structure, and Yb prefers a fcc structure. These all agree with experiments. Using the standard potential (see Table I, footnote a) makes the energies of various lattices anomalously large compared with the other REs. The bcc lattice has a surprisingly high energy, considering that it is stable at high temperatures. This may be due to the fact that the bcc lattices of many pure elements such as Pm,<sup>32</sup> Ti,<sup>34–36</sup> Zr,<sup>37</sup> and others<sup>38</sup> are mechanically unstable. They are stabilized at high temperatures only by thermal fluctuations. We believe that this is the case for all REs with exception of Eu and Yb. In fact, a previous study by Gao *et al.*<sup>32</sup> confirmed mechanical instability of both Pm.cI2 and Ac.cI2. We checked the vibrational modes for Yb.cI2 and found that it is stable, in agreement with the fact that both Eu and Yb prefer a bcc lattice in equilibrium at all temperatures in the solid state.

We also compare the enthalpies obtained in this study with that of a previous FP report by Wang *et al.*<sup>9</sup> who used high precision generalized gradient approximation (GGA) potentials and a plane-wave energy cutoff 1.75 times the default one for selected lattices of fcc, bcc, and hcp of pure elements and another report by Sluiter<sup>16</sup> who used high precision and GGA potentials for lattices of fcc, bcc, and uncommon complex of pure elements. For all the REs, the enthalpy data from these three independent studies are very close, with most within  $\pm 0.5$  kJ/mol, suggesting that medium precision and default plane-wave energy cutoff are adequate and appropriate for enthalpy calculations.<sup>18</sup> Also, we find little difference in the calculated energy from GGA and PBE potentials.

To verify our ability to calculate lattice parameters, we compare the calculated volume at  $T=0$  K with the corresponding data of the stable structure of each RE element at SER state [see Fig. 1(b)]. The predicted volume at 0 K agrees well with experimental data at 298 K except for Ce. Using the standard Ce potential correctly predicts the remarkable volume collapse of Ce, while using the Ce<sub>3</sub> po-

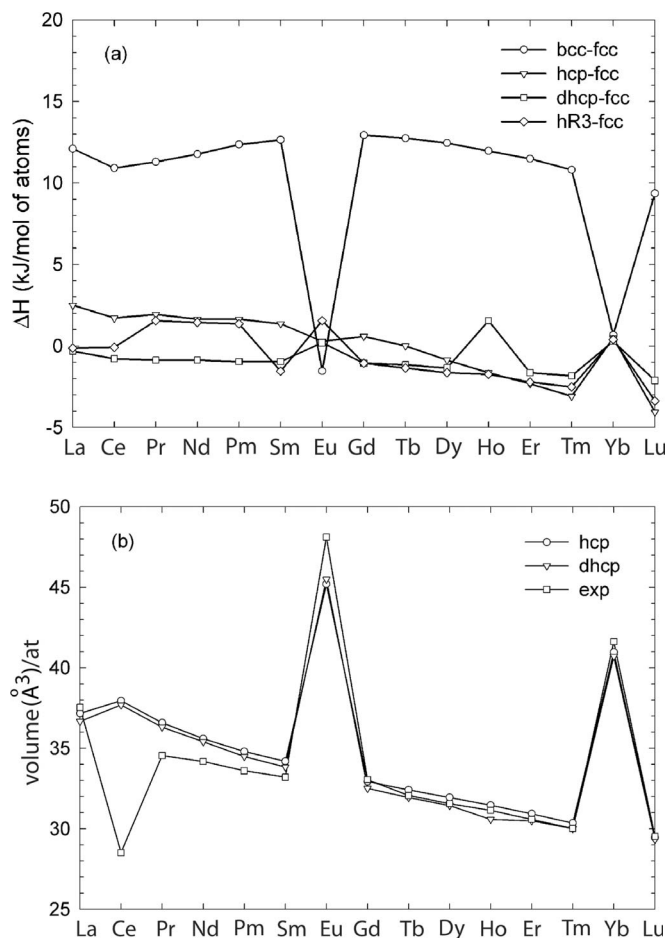


FIG. 1. (a) The enthalpy of various (stable and hypothetical) lattice structures of RE elements in bcc (cI2), hcp (hP2), dhcp (hP4), and hR3 with respect to fcc (cF4) lattice at the ground state at 0 K calculated in this study. (b) The calculated atomic volume of RE elements in hcp and dhcp structures. The experimental data are the volume of the stable structure at 1 atm and 298 K, calculated based on the lattice parameters presented in Ref. 20.

tential fails. In either case, the calculated lattice parameter disagrees with experimental values. The drastic change in lattice parameters and energy when switching between the standard Ce and Ce<sub>3</sub> potentials suggests that the potentials for cerium (Ce or Ce<sub>3</sub>) are not optimal or else reveals an intrinsic failure of density-functional theory. Note the overall decrease in volume per atom across the RE series caused by increasing nuclear charge (except the anomalous volume expansion of Eu and Yb compared with their neighbor elements). We refer to this effect as the “lanthanide contraction.”<sup>22,23</sup>

## B. Al-early RE binaries (Figure 2)

### 1. Al-La [Figure 2(a)]

Our calculations on the Al-La system show an excellent agreement with experiments<sup>20,21</sup> and another FP report.<sup>39</sup>  $\text{Al}_{11}\text{La}_3$ .oI28,  $\text{Al}_3\text{La}$ .hP8,  $\text{Al}_2\text{La}$ .cF24, and  $\text{AlLa}$ .oC16 all lie on the convex hull, and they are all known stable phases.<sup>20,21</sup>  $\text{Al}_4\text{La}$ .tI10 and  $\text{AlLa}_3$ .hP8 lie above the convex

TABLE II. Enthalpies of a variety of  $Al_xRE_y$  compounds calculated from FP at  $T=0$  K. The unit is kJ/mol of atoms.

Phase	Structure	La	Ce <sub>3</sub> (Ce) <sup>a</sup>	Pr <sub>3</sub>	Nd <sub>3</sub>	Pm <sub>3</sub>	Sm <sub>3</sub>	Eu <sub>2</sub>	Gd <sub>3</sub> (Gd) <sup>b</sup>	Tb <sub>3</sub>	Dy <sub>3</sub>	Ho <sub>3</sub>	Er <sub>3</sub>	Tm <sub>3</sub>	Yb <sub>2</sub> (Yb) <sup>c</sup>	Lu <sub>3</sub>
Al <sub>4</sub> RE	Al <sub>4</sub> U.oI20	-33	-32(-32)	-33	-33	-34	-34	-20	-33(-34)	-33	-33	-32	-31	-30	-17(-23)	-29
Al <sub>4</sub> RE	Al <sub>4</sub> Ba.tI10	-35	-30(-28)	-30	-29	-28	-27	-29	-25(-27)	-24	-23	-22	-20	-19	-20(-21)	-16
Al <sub>11</sub> RE <sub>3</sub>	Al <sub>11</sub> La <sub>3</sub> .oI28	-39	-36(-34)	-36	-36	-36	-35	-26	-33	-33	-32	-31	-30	-29	-22(-21)	-27
Al <sub>3</sub> RE	AuC <sub>3</sub> .cP4	-30	-30(-35)	-34	-36	-37	-38	-14	-40	-41	-41	-40	-40	-40	-17(-29)	-38
Al <sub>3</sub> RE	Ni <sub>3</sub> Sn.hp8	-44	-43(-40)	-44	-43	-44	-43	-24	-42(-42)	-42	-42	-41	-40	-19	-20(-28)	-37
Al <sub>3</sub> RE	Ni <sub>3</sub> Ti.hp16	-35	-35(-36)	-38	-39	-40	-40	-16	-42	-42	-42	-41	-41	-40	-18(-28)	-18
Al <sub>3</sub> RE	BaPb <sub>3</sub> .hR12	-39	-39(-38)	-40	-41	-42	-41	-20	-41(-41)	-41	-41	-40	-40	-39	-19(-28)	-37
Al <sub>3</sub> RE	Al <sub>3</sub> Ho.hR20	-32	-34(-35)	-39	-40	-41	-41	-16	-42	-42	-41	-41	-40	-39	-18	-37
Al <sub>2</sub> RE	Cu <sub>2</sub> Mg.cF24	-49	-46(-44)	-48	-49	-49	-50	-38	-50(-51)	-51	-50	-49	-49	-48	-34(-40)	-46
Al <sub>2</sub> RE	AlB <sub>2</sub> .hP3	-45	-44(40)	-46	-46	-47	-47	-29	-47	-48	-47	-47	-46	-45	-26	-44
AIRE	ClCs.cP2	-35	-31(-23)	-33	-34	-35	-36	-19	-38(-38)	-38	-38	-38	-38	-37	-18	-36
AIRE	BCr.oC8	-33	-33(-19)	-33	-34	-34	-35	-22	-36	-37	-37	-36	-37	-37	-20	-36
AIRE	AlCe.oC16	-40	-37(-30)	-38	-38	-39	-39	-27	-40(-40)	-40	-40	-39	-39	-39	-22	-38
AIRE	AlDy.oP16	-40	-36(-31)	-37	-38	-39	-39	-27	-40(-41)	-40	-40	-40	-40	-40	-23	-39
AIRE	AlEu.oP20	-35	-34(-26)	-35	-35	-36	-36	-29	-37	-37	-37	-36	-36	-35	-24	-34
Al <sub>2</sub> RE <sub>3</sub>	Si <sub>2</sub> U <sub>3</sub> .10	-26	-24(-10)	-26	-26	-25	-27	-13	-28	-29	-29	-29	-29	-29	-11	-29
Al <sub>2</sub> RE <sub>3</sub>	Al <sub>2</sub> Gd <sub>3</sub> .tP20	-28	-25(-17)	-27	-27	-28	-28	-20	-30(-34)	-31	-31	-31	-32	-32	-17	-32
AIRE <sub>2</sub>	Co <sub>2</sub> Si.oP12	-25	-21(-21)	-23	-24	-25	-25	-15	-27(-28)	-28	-28	-28	-29	-28	-12	-28
AIRE <sub>2</sub>	Al <sub>2</sub> Cu.tI12	-23	-20(-13)	-20	-19	-19	-18	-10	-18	-18	-16	-17	-16	-20	-8	-20
AIRE <sub>3</sub>	AuC <sub>3</sub> .cP4	-18	-15(-15)	-16	-16	-16	-16	-5	-18	-18	-18	-18	-18	-18	-2	-18
AIRE <sub>3</sub>	Ni <sub>3</sub> Sn.hp8	-20	-16(-15)	-17	-17	-18	-18	-10	-19	-19	-19	-19	-20	-19	-6	-19
AIRE <sub>3</sub>	AlCe <sub>3</sub> .mP16	-20	-15(-16)	-17	-17	-18	-17	-11	-18	-19	-19	-19	-19	-19	-8	-19

<sup>a</sup>The value in parenthesis was obtained using the standard Ce potential, considering collinear magnetism only.

<sup>b</sup>The value in parenthesis was obtained using the standard Gd potential, considering collinear magnetism only.

<sup>c</sup>The value in parenthesis was obtained using the standard Yb potential, considering collinear magnetism only.

hull by 1.4 and 0.2 kJ/mol, respectively, and both are known as high-temperature phases.<sup>20,21,40</sup>

The so-called Al<sub>5</sub>La<sub>2</sub>.hP3 was first identified by Buschow<sup>40</sup> who found that it was stable only over a narrow temperature range of 1090–1240 °C. He assigned it a chemistry of Al<sub>2.4</sub>La (~29.3 at. % La) and suggested a mutual substitution between Al and La on both the 1a and 2d Wyckoff sites. The exact occupancy fraction of each element was not determined. We find that the stoichiometric variant is unstable by 3.5 kJ/mol. In order to calculate the energy of Al<sub>5</sub>La<sub>2</sub>.hP3, we built a 2 × 2 × 2 supercell of Al<sub>2</sub>La.hP3 and then substituted one Al atom or vacancy for La to reach a composition close to Al<sub>5</sub>La<sub>2</sub>. Substitution of one vacancy for La results in an energy above the convex hull by 14.1 kJ/mol, substitution of one Al atom for La energy above the convex hull by 9.8 kJ/mol, and substitution of one vacancy for Al energy above the convex hull by 8.4 kJ/mol. We conclude that both substitution and vacancy energies are too high to stabilize the Al<sub>5</sub>La<sub>2</sub>.hP3 phase at high temperatures. What remains equally questionable is whether the Al<sub>5</sub>La<sub>2</sub>.hP3 phase should be treated as stoichiometric at all as treated in Refs. 20, 21, and 40, since its exact composition remains unknown to date. More careful theoretical and experimental studies on the stability of Al<sub>5</sub>La<sub>2</sub>.hP3, especially its atomic occupancy and homogeneity range, would be desirable to fix the Al-La binary phase diagram. The possible presence of Al<sub>5</sub>La<sub>2</sub>.hP3 in Al-La raises the question of why

the same structure is not reported in other Al-RE such as Al-Ce.

## 2. Al-Ce, Al-Pr, Al-Nd, Al-Pm, and Al-Sm [Figures. 2(b)–2(f)]

The experimental phase diagrams<sup>20,21</sup> and the calculated  $T=0$  K enthalpies (see Table II) for Al-Ce, Al-Pr, Al-Nd, Al-Pm, and Al-Sm are similar to each other and also similar to Al-La. Both Al<sub>3</sub>RE.hp8 and Al<sub>2</sub>RE.cF24 are correctly predicted to be stable, while Al<sub>4</sub>RE.oI20 and Al<sub>11</sub>RE<sub>3</sub>.oI28 just lie slightly above the convex hull. The energies of Al-RE.oC16 and AIRE.oP16 are almost equal within the uncertainty of this calculation. They lie on the convex hull for RE=La,Pr,Nd,Sm, while experiments find that they are stable for RE=La,Ce,Pr, so we correctly predict the *trend* of stability for early RE, but not the exact *range* of stability. Experimentally, AIRE<sub>2</sub>.oP12 is stable for these systems but its calculated energy lies slightly above the convex hull. Similarly, AIRE<sub>3</sub>.hp8 is known to be stable for RE=La,Ce,Pr,Nd, but its energy all lies above the convex hull. The competing structure AIRE<sub>3</sub>.cP4 is known to be stable at high temperature for RE=Ce,Pr, and our calculations confirm that its energy is greater than that of hp8. In short, the agreement with experimental phase diagram<sup>20,21</sup> is nearly perfect for Al-rich compounds but not for RE-rich compounds. We think that this is most probably due to the use of an approximate exchange-correlation potential while tightly bound  $f$  electrons may exhibit strong correlations.<sup>12</sup>

TABLE III. Enthalpies of stable  $\text{Al}_x\text{RE}_y$  compounds obtained from experimental measurements (kJ/mol of atoms). All data from Refs. 56, 57, and 60 are from emf measurements. The experimental uncertainty varies between  $\pm 0.4$  and  $\pm 12.1$  kJ/mol of atoms (most under  $\pm 5.0$  kJ/mol). The uncertainty from Ref. 58 is  $\pm 2$  kJ/mol of atoms.

Phase	La	Ce	Pr	Nd	Sm	Eu	Gd	Tb	Dy	Ho	Er	Tm	Yb
$\text{Al}_4\text{La.tI10}$	-37.5 <sup>a</sup>												
$\text{Al}_{11}\text{RE}_3.\text{oI28}$	-42.7 <sup>b</sup>	-41 <sup>c</sup>	-46 <sup>d</sup>	-38.7 <sup>e</sup>									
	-41.0 <sup>f</sup>	-39.5 <sup>g</sup>	-43 <sup>h</sup>										
	-41 <sup>i</sup>												
$\text{Al}_3\text{RE.cP4}$													-32.5 <sup>j</sup> -32.5 <sup>f</sup>
$\text{Al}_3\text{RE.hp8}$	-52.3 <sup>b</sup>	-48 <sup>k</sup>	-54 <sup>d</sup>	-45 <sup>e</sup>	-48.0 <sup>l</sup>		-46.5 <sup>m</sup>						
	-44.0 <sup>f</sup>						-43.4 <sup>n</sup>						
$\text{Al}_2\text{RE.cF24}$	-47.1 <sup>i</sup>	-50 <sup>c</sup>	-54 <sup>o</sup>	-53 <sup>e</sup>	-54.3 <sup>o</sup>	-36 <sup>o</sup>	-63.6 <sup>m</sup>	-52.4 <sup>o</sup>	-52.7 <sup>o</sup>	-52.5 <sup>o</sup>	-49.1 <sup>g</sup>	-51.0 <sup>o</sup>	-38.2 <sup>o</sup>
	-54.2 <sup>o</sup>	-48.9 <sup>g</sup>	-71 <sup>d</sup>	-53.6 <sup>o</sup>	-55.0 <sup>l</sup>		-51.4 <sup>g</sup>				-50.5 <sup>o</sup>		-36.4 <sup>i</sup>
	-49.9 <sup>p</sup>	-50 <sup>k</sup>	-53 <sup>h</sup>				-53.2 <sup>n</sup>						-39.5 <sup>f</sup>
	-50.5 <sup>f</sup>	-52.2 <sup>o</sup>											
	-67.0 <sup>b</sup>												
$\text{AlRE.oC16}$	-83.3 <sup>b</sup>	-46 <sup>c</sup>											
	-45.9 <sup>f</sup>	-78 <sup>k</sup>											
$\text{AlRE.oP16}$			-99 <sup>d</sup>	-50 <sup>e</sup>	-49.0 <sup>l</sup>		-86.6 <sup>m</sup>						
			-47 <sup>h</sup>				-39.4 <sup>g</sup>						
							-42.9 <sup>n</sup>						
$\text{Al}_2\text{RE}_3.\text{tP20}$							-98.3 <sup>m</sup>						
							-33.3 <sup>n</sup>						
$\text{AlRE}_2.\text{oP12}$			-111 <sup>d</sup>	-36.5 <sup>e</sup>	-38.0 <sup>l</sup>		-89.5 <sup>m</sup>						
			-33 <sup>h</sup>				-34.7 <sup>g</sup>						
							-29 <sup>n</sup>						
$\text{AlRE}_3.\text{hp8}$	-49.4 <sup>b</sup>	-27 <sup>c</sup>	-99 <sup>d</sup>	-27.5 <sup>e</sup>									
	-25.0 <sup>i</sup>	-16.4 <sup>g</sup>	-24.9 <sup>h</sup>										
	-26.5 <sup>f</sup>	-77 <sup>k</sup>											

<sup>a</sup>Reference 55.

<sup>b</sup>Reference 56.

<sup>c</sup>Reference 45.

<sup>d</sup>Reference 57.

<sup>e</sup>Reference 46.

<sup>f</sup>Reference 47.

<sup>g</sup>Reference 51.

<sup>h</sup>Reference 58.

<sup>i</sup>Reference 52.

<sup>j</sup>Reference 59.

<sup>k</sup>Reference 60.

<sup>l</sup>Reference 48.

<sup>m</sup>Reference 61.

<sup>n</sup>Reference 62.

<sup>o</sup>Reference 53.

<sup>p</sup>Reference 63.

Both the Al-Ce and Al-Nd systems were discussed in our previous publication.<sup>12</sup> That study considered spin polarization with collinear magnetization using “accurate” precision and the standard Ce and Nd potentials. The enthalpy data for all the stable compounds in this study agree with an early report<sup>12</sup> within  $\pm 3$  kJ/mol, except  $\text{AlNd}_3.\text{hp8}$  whose energy is higher by +10 kJ/mol in this paper. The consistency of enthalpies using different potentials gives one measure of accuracy of our results.

The phase diagram of Al-Pm is not known experimentally. Detailed descriptions comparing the Pm<sub>3</sub> and Pm potentials and considering magnetic structures are described in our recent report.<sup>32</sup> Pm is an early lanthanide element, located between Nd and Sm in the Periodic Table, so it is reasonable to suppose that the Al-Pm phase diagram may be similar to that of Al-Sm and/or Al-Nd as we confirm in Fig. 2. In particular, the energies of the  $\text{Al}_3\text{Pm.hp8}$ ,  $\text{Al}_2\text{Pm.cF24}$ , and  $\text{AlPm.oC16}$  lattices are all located on the convex hull. It

is noteworthy that the  $\text{AlPm.oP16}$  structure has a slightly higher energy (by 0.4 kJ/mol) than  $\text{AlPm.oC16}$ , which is well within the uncertainty of our calculations. Therefore, an unambiguous statement on the relative stability between  $\text{AlPm.oP16}$  and  $\text{AlPm.oC16}$  cannot be made, and calculations of their vibrational free energies at finite temperatures are desirable. As a matter of fact,  $\text{AlRE.oP16}$  appears experimentally to be stable in both the Al-Nd and Al-Sm systems.<sup>20,21,33</sup>

### 3. Al-Eu [Figure 2(g)]

The Al-Eu system is very different from its neighboring Al-RE systems because it only has three compounds identified namely,  $\text{Al}_4\text{Eu.tI10}$ ,  $\text{Al}_2\text{Eu.cF24}$ , and  $\text{AlEu.oP20}$ ,<sup>20,21</sup> which is referred to as  $\text{AlEu.oP18}$  in Refs. 20 and 21. Note that the Al-Eu phase diagram, especially the portion relating to the liquid, is not completely established yet.<sup>20,21</sup> Our calculations on the Al-Eu system agree excellently with experiments. All three stable phases are predicted to be stable un-

TABLE IV. Comparison in lattice stability between experiments (Refs. 12, 20, and 21), which is marked with letters, and the present FP calculation at 0 K, which is marked with symbols in parentheses. Letter “S” means a stable phase, “HT” means a high-temperature phase, “LT” means a low-temperature phase, and unmarked phase means an unstable phase according to Refs. 20 and 21. The symbol (✓) means a phase on the convex hull or above by less than 0.5 kJ/mol, (◇) means that a phase is above the convex hull by less than 2 kJ/mol, and unmarked phase means that a phase lies above the convex hull by more than 2 kJ/mol. The structural information is not yet reported in Refs. 20 and 21.

Phase	La	Ce <sub>3</sub>	Pr <sub>3</sub>	Nd <sub>3</sub>	Pm <sub>3</sub>	Sm <sub>3</sub>	Eu <sub>2</sub>	Gd <sub>3</sub>	Tb <sub>3</sub>	Dy <sub>3</sub>	Ho <sub>3</sub>	Er <sub>3</sub>	Tm <sub>3</sub>	Yb <sub>2</sub>	Lu <sub>3</sub>
Al <sub>4</sub> RE.oI20			(◇)	(◇)	(◇)	(◇)		(◇)	(◇)	(◇)	(◇)	(◇)	(◇)		
Al <sub>4</sub> RE.tI10	HT(◇)	HT	HT	HT		HT	S(✓)								(✓)
Al <sub>11</sub> RE <sub>3</sub> .oI28	LT(✓)	LT(◇)	LT(◇)	LT(◇)	(◇)	(◇)									(✓)
Al <sub>3</sub> RE.cP4									(◇)	(◇)	(◇)	S(✓)	S(✓)	S	S(✓)
Al <sub>3</sub> RE.hp8	S(✓)	LT(✓)	S(✓)	LT(✓)	(✓)	S(✓)		S(✓)	(✓)	(✓)	(◇)	(◇)	(◇)		(◇)
Al <sub>3</sub> RE.hp16								(◇)	(◇)	LT(✓)	(✓)	(✓)	(✓)		(✓)
Al <sub>3</sub> RE.hp12		HT		HT		(◇)		(◇)	S(✓)	(✓)	(◇)	(◇)	(◇)		(◇)
Al <sub>3</sub> RE.hR20								(◇)	(◇)	HT(✓)	S(✓)	(✓)	(✓)		(✓)
Al <sub>2</sub> RE.cF24	S(✓)	S(✓)	S(✓)	S(✓)	(✓)	S(✓)									
Al <sub>2</sub> RE.hp3	HT	(◇)	(◇)												
AIRE.cP2									(◇)						
AIRE.oC8															
AIRE.oC16	S(✓)	S(✓)	HT(✓)	(✓)	(✓)	(✓)		(✓)	(◇)	(◇)	(◇)	(◇)	(◇)		(◇)
AIRE.oP16	(◇)	(◇)	LT(◇)	S(✓)	(✓)	S(✓)		S(✓)	S(✓)	S(✓)	S(✓)	S(✓)	S(✓)		S(✓)
AIRE.oP20								S(✓)							(◇)
Al <sub>2</sub> RE <sub>3</sub> .tP10															
Al <sub>2</sub> RE <sub>3</sub> .tP20								S	S(◇)	S(◇)	S(◇)	S(◇)	S(◇)		S(◇)
AIRE <sub>2</sub> .oP12	(◇)	HT	S	S(◇)	(◇)	S(◇)		S(✓)	S(✓)	S(✓)	S(✓)	S(✓)	S*	(✓)	S(✓)
AIRE <sub>2</sub> .tI12															
AIRE <sub>3</sub> .cP4		HT	HT												
AIRE <sub>3</sub> .hp8	S(✓)	LT	LT	S(◇)	(◇)	(◇)		(◇)	(◇)	(◇)	(◇)				
AIRE <sub>3</sub> .mP16	(✓)						(◇)	(◇)	(◇)						

equivocally because all other hypothetical compounds lie far above the convex hull. AlEu.oP20 is reported as a stable structure for Eu but not for any other REs. To ascertain whether AlEu.oP20 or AlEu.oP18 is the stable structure in Al-Eu, we check the possibility of vacancy substitution in AlEu.oP20 to form the AlEu.oP18 structure. There are three Wyckoff sites for Al ( $2a, 4e, 4f$ ) and three sites for Eu ( $2b, 4e, 4e$ ) in the AlEu.oP20 lattice. Substituting a vacancy into the Al and Eu site, respectively, in a unit cell of AlEu.oP20 lattice to reach the composition of AlEu.oP18 suggests that there are nine different atomic configurations allowed. We examined the total energies of all nine possible structures and found that they all exceed the fully occupied oP20 structure by 9.6 kJ/mol or more, suggesting that vacancy substitution to form AlEu.oP18 is unlikely.

### C. Al-late RE binaries (Figure 3)

#### 1. Al-Gd [Figure 3(a)]

Except for Al<sub>2</sub>Gd<sub>3</sub>.tP20, our calculations on the Al-Gd system agree very well with experiments.<sup>20,21</sup> Four phases are predicted to be stable, namely, Al<sub>3</sub>Gd.hp8, Al<sub>2</sub>Gd.cF24, AlGd.oP16, and AlGd<sub>2</sub>.oP12, which all are experimentally

proven to be stable,<sup>20,21</sup> while the energy of stable Al<sub>2</sub>Gd<sub>3</sub>.tP20 lies above the convex hull by 2.0 kJ/mol. Using the standard Gd potential (see Table II), we find that Al<sub>2</sub>Gd<sub>3</sub>.tP20 correctly lies on the convex hull. Similarly, the standard Gd potential correctly predicts the thermal stability of elemental Gd, while using Gd<sub>3</sub> fails (see Table I). Differences in enthalpy due to the choice of potential are strikingly small, all within 1–2 kJ/mol, except for 4 kJ/mol for Al<sub>2</sub>Gd<sub>3</sub>.tP20 (see Table II).

Note that the energies of AlGd.oC16 and AlGd.oP16 are nearly equal; thus, an entropy effect must be responsible for the experimental observation that only AlGd.oP16 is stable above room temperature.<sup>20,21</sup> Al<sub>4</sub>Gd (prototype Al<sub>4</sub>U.oI20) lies above the convex hull by 0.7 kJ, implying that it could become stable at high temperatures or by impurity or pressure effects. The Al<sub>3</sub>Gd family (hp8, hp16, hR13, and hR20) all have comparable energies, so we suggest that future experimental or theoretical studies examine the possibility in allotropes of the Al<sub>3</sub>Gd family at high temperatures.

#### 2. Al-Tb, Al-Dy, Al-Ho, Al-Er, Al-Tm, and Al-Lu [Figures 3(b)–3(g)]

For the late RE systems (except Yb), our calculations predict lattice stabilities that resemble the Al-Gd system.

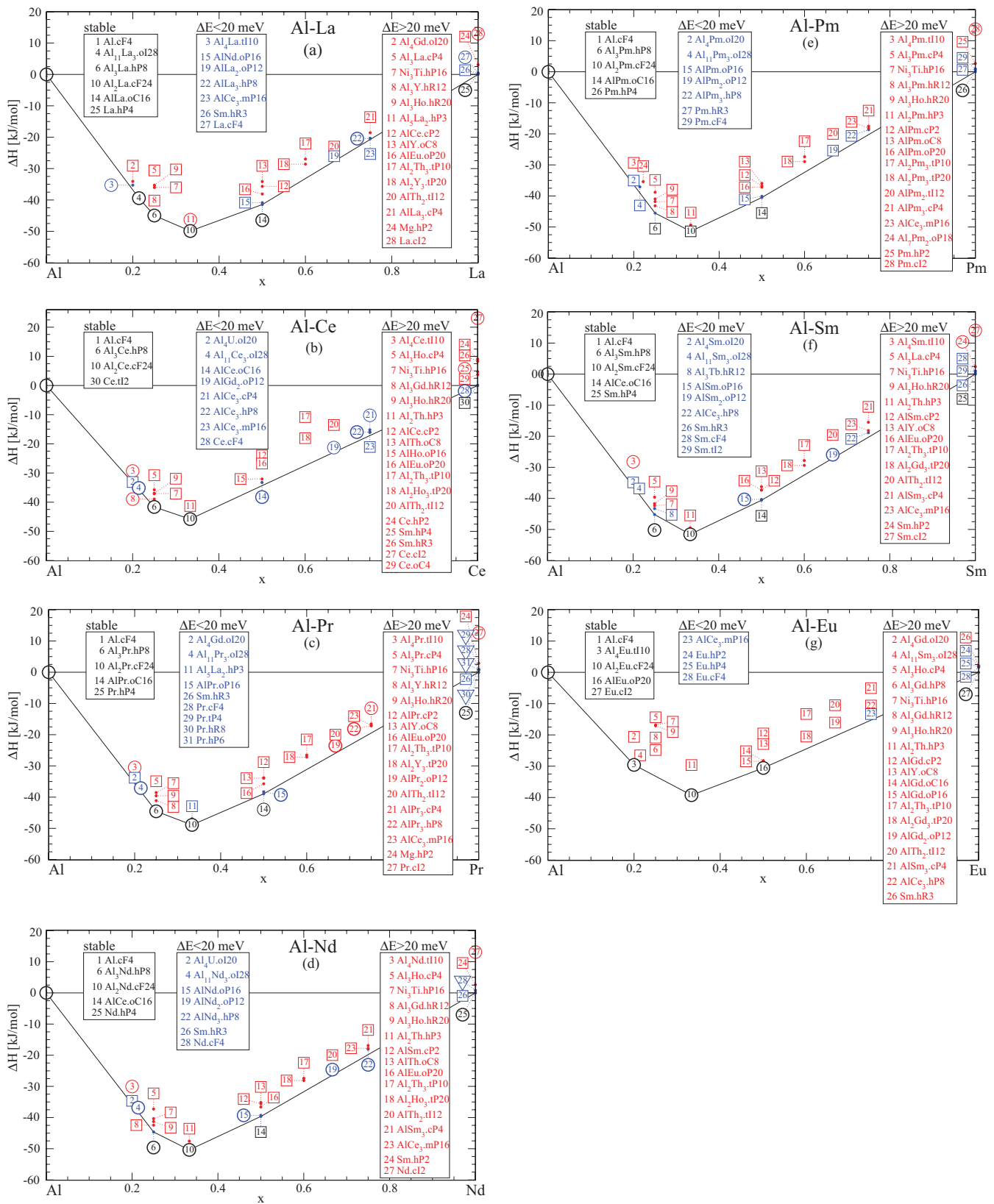


FIG. 2. (Color online) The convex hull plots of the enthalpies of formation of Al-early RE (i.e., La, Ce, Pr, Nd, Pm, Sm, and Eu) binary systems calculated at 0 K. See the text for details about the choice of potentials. The plotting symbol notations are (black or blue) heavy circles for known stable binary phases, (red or blue) light circles for known high-temperature phases, (blue) triangles for known high-pressure phases, and (red, blue, or black) squares for imperfectly known, unknown, or hypothetical structures. Tie-lines run along convex hull edges, joining low enthalpy structures at the vertices of the convex hull.

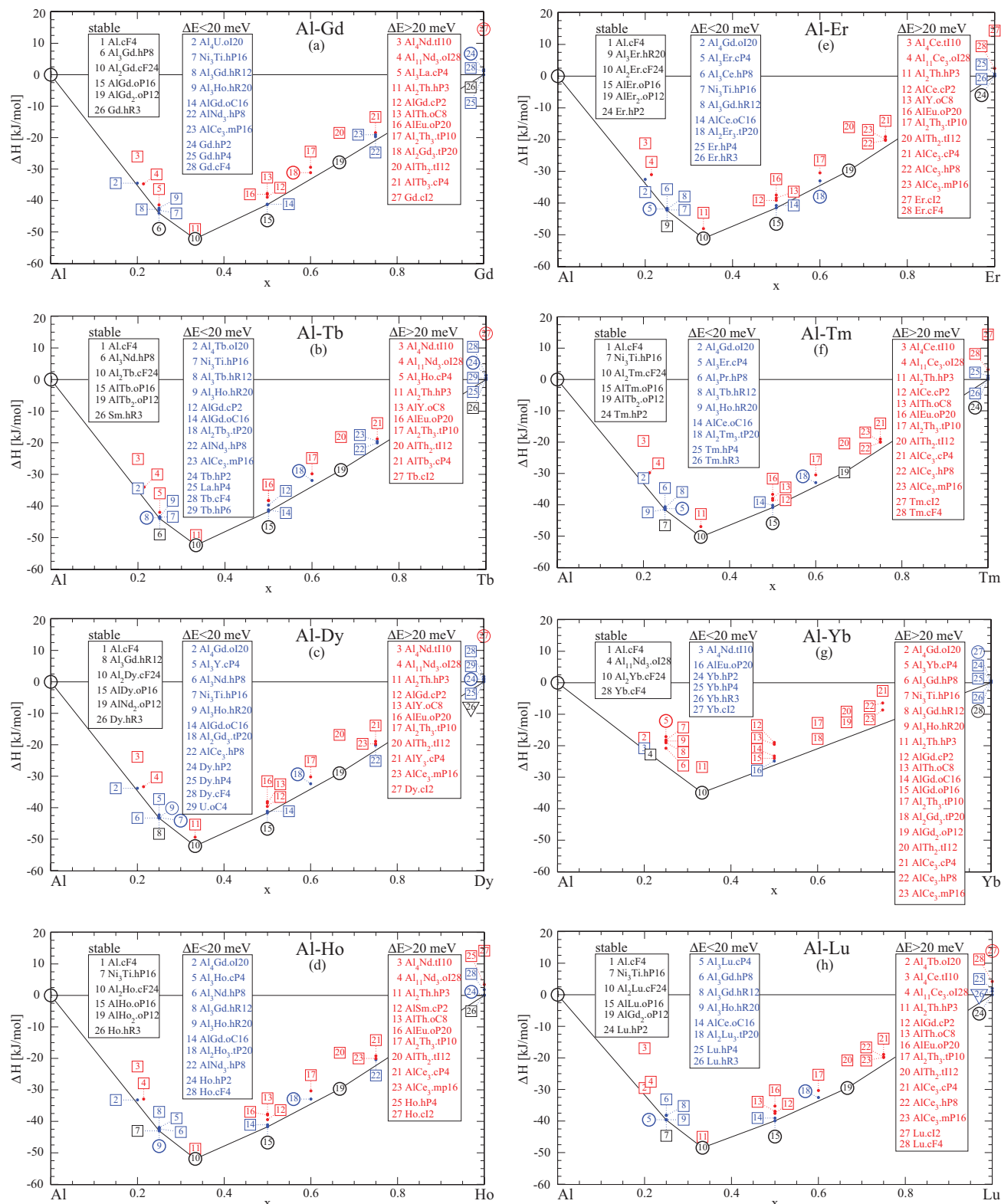


FIG. 3. (Color online) The convex hull plots of the enthalpies of formation of Al-late RE (i.e., Gd, Tb, Dy, Ho, Er, Tm, Yb, and Lu) binary systems calculated at 0 K. Plotting symbols are as in Fig. 2.

Their convex hull plots are shown in Figs. 3(b)–3(g), respectively. One common feature is that  $\text{Al}_2\text{RE}.\text{cF24}$ ,  $\text{AlRE}.\text{oP16}$ , and  $\text{AlRE}_2.\text{oP12}$  all lie on the convex hull, all of which prove experimentally to be stable.<sup>20,21</sup> Note that there are several allotropes of the  $\text{Al}_3\text{RE}$  family whose energy differs

marginally, namely,  $\text{cP4}$ ,  $\text{hP8}$ ,  $\text{hR12}$ ,  $\text{hP16}$ , and  $\text{hR20}$ , suggesting a high possibility that allotropes exist in this family. In fact, it is reported that an allotropic transition of  $\alpha\text{Al}_3\text{Dy}.\text{hP16} \leftrightarrow \beta\text{Al}_3\text{Dy}.\text{hR20}$  occurs at 1005 °C in Al-Dy.<sup>20</sup>

As in the case of Al-Gd,  $\text{Al}_2\text{RE}_3$ .tP20 is stable experimentally for late trivalent RE elements, but our calculation finds its energy slightly above the convex hull. We presume that the error is due to the lack of magnetism in the trivalent RE<sub>3</sub> potential, which affects  $\text{Al}_2\text{RE}_3$ .tP20 more strongly than other structures (e.g., see Al-Gd in Table II). Unfortunately, for Tb, Dy, Ho, and Er, only trivalent potentials are provided with VASP.

The crystal structure of  $\text{AlTm}_2$  is not known in Refs. 20 and 21, and we predict it to be  $\text{AlTm}_2$ .oP12 (prototype  $\text{Co}_2\text{Si}$ ), consistent with other late REs.

### 3. Al-Yb [Figure 3(h)]

The Al-Yb system differs significantly from the previous systems. First, there are only two stable compounds known in the system,<sup>20,21</sup> namely,  $\text{Al}_3\text{Yb}$ .cP4 and  $\text{Al}_2\text{Yb}$ .cF24. Interestingly, only  $\text{Al}_2\text{Yb}$ .cF24 is confirmed stable at 0 K in our calculations, while the reported  $\text{Al}_3\text{Yb}$ .cP4 lies above the convex hull by 9.0 kJ, allowing  $\text{Al}_{11}\text{Yb}_3$ .oI28 to lie on the convex hull. Calculation using the standard Yb potential considering collinear magnetism only finds that the  $\text{Al}_3\text{Yb}$ .cP4 lies above the convex hull by 1.4 kJ, which implies that it is possible that  $\text{Al}_3\text{Yb}$ .cP4 becomes stable by vibrational free energy at high temperature. Further including spin-orbital coupling with standard Yb potential does not impact the Al-Yb lattice stability significantly.

## IV. SYSTEMATICS AND ANOMALIES IN ENTHALPIES OF FORMATION (FIGURE 4)

Classified by compound chemistry, we identify seven families of Al-RE compounds, namely,  $\text{Al}_4\text{RE}$ ,  $\text{Al}_3\text{RE}$ ,  $\text{Al}_2\text{RE}$ ,  $\text{AlRE}$ ,  $\text{Al}_2\text{RE}_3$ ,  $\text{AlRE}_2$ , and  $\text{AlRE}_3$ . For each family, several allotropes compete for phase stability. Since the RE elements change their electronic configuration across the Periodic Table (e.g., the number of  $4f$  orbital electrons, volume, and atomic radius), we would expect both systematics and anomalies as already discussed by Buschow and Vanvucht<sup>41</sup> and Gschneidner.<sup>23,42–44</sup> Most of the enthalpies cited by Gschneidner<sup>42</sup> were obtained using electromotive force (emf) method and thus may be less reliable than those obtained more recently using calorimetry (see Table III). Experimental data on the Al-early RE (up to Al-Sm) is relatively complete, thanks to the consistent data set from Borzone *et al.*<sup>45–50</sup> and from the Keita and co-workers.<sup>51,52</sup> On the other hand, there are no experimental reports on the formation enthalpies of the compounds for the Al-late RE or for Al-Eu except Al-Gd, Al-Yb, and  $\text{Al}_2\text{RE}$ .cF24.<sup>53</sup> Al-Pm and Al-Lu are not listed in Table III since no reports can be found. In this section, we compare the calculated enthalpy data with those from available experiments and examine trends in stability across the RE series.

### A. $\text{Al}_4\text{RE}$ family (oI20, tI10, and oI28) [Figure 4(a)]

The  $\text{Al}_4\text{RE}$ .oI20,  $\text{Al}_4\text{RE}$ .tI10, and  $\text{Al}_{11}\text{RE}_3$ .oI28 compounds are close in composition and they compete for stability. Therefore, they do not coexist in equilibrium over a wide temperature range. Rather, oI28 is stable at low temperatures and tI10 is stable at high temperatures in Al-early RE sys-

tems.  $\text{Al}_4\text{RE}$ .tI10 and  $\text{Al}_{11}\text{RE}_3$ .oI28 are not allotropes (i.e., polymorphous transformation) since their compositions differ, and this has been recently demonstrated by Gao *et al.*<sup>12</sup> using differential scanning calorimetry measurements. Calculated enthalpies of formation of tI10 and oI28 across the Periodic Table are shown in Fig. 4. Our calculations correctly predict that  $\text{Al}_4\text{RE}$ .tI10 is unstable with respect to  $\text{Al}_4\text{RE}$ .oI20 and  $\text{Al}_{11}\text{RE}_3$ .oI28 in all case except for La, Eu, and Yb. The overall trend is that, with increasing atomic number of the RE series, the formation enthalpy for all three types of compounds increases (toward positive direction) steadily. Exceptions occur at Eu and Yb.  $\text{Al}_4\text{Eu}$ .tI10 has the lowest energy among the  $\text{Al}_4\text{RE}$  family in Al-Eu, and actually it is stable all the way up to its melting point. On the other hand,  $\text{Al}_4\text{Yb}$ .tI10 is more stable than  $\text{Al}_4\text{Yb}$ .oI20 but less stable than  $\text{Al}_{11}\text{Yb}_3$ .oI28.

### B. $\text{Al}_3\text{RE}$ family (cP4, hP8, hP16, hR12, and hR20) [Figure 4(b)]

Figure 4(b) shows that, for early REs including Eu, the energies of the five  $\text{Al}_3\text{RE}$  allotropes vary in a wide range, but  $\text{Al}_3\text{RE}$ .hP8 remains the most stable in agreement with experiments.<sup>20,21</sup> For the RE after Eu, the energies of all five  $\text{Al}_3\text{RE}$  allotropes become nearly degenerate. Again, Eu and Yb provide exceptions, where the energy of all five allotropes rises by roughly 50%. The overall trend is that  $\text{Al}_3\text{RE}$ .hP8 is favored for early REs while  $\text{Al}_3\text{RE}$ .cP4 and  $\text{Al}_3\text{RE}$ .hP16 are favored for late elements except for Eu and Yb. Allotropes are observed experimentally for Ce, Nd, and Dy. We suggest experiments to investigate their occurrence in the case of all RE elements, especially the late RE elements Gd-Lu (except Yb).

### C. $\text{Al}_2\text{RE}$ family (cF24 and hP3) [Figure 4(c)]

$\text{Al}_2\text{RE}$ .cF24 has the lowest enthalpy compared to all other compounds in each system, implying that the strongest interatomic bonding occurs in this cF24 structure. Indeed,  $\text{Al}_2\text{RE}$ .cF24 has the highest melting point in all the Al-RE binary phase diagrams.<sup>20,21</sup> It melts congruently and it has large impact on the shape of the Al-RE phase diagrams.<sup>20,21</sup> Enthalpies for all the  $\text{Al}_2\text{RE}$ .cF24 structures fluctuate within a narrow range except for Ce and especially Eu and Yb, where the absolute enthalpy data are much smaller (in other words, much weaker bonding). In fact, the melting point of  $\text{Al}_2\text{Eu}$  and  $\text{Al}_2\text{Yb}$  is lower by more than 100 °C compared to their neighbor  $\text{Al}_2\text{RE}$  compounds [see Fig. 5(b)].

On the other hand, the so-called  $\text{Al}_3\text{La}_2$ .hP3 actually has a stoichiometry of  $\text{Al}_2\text{RE}$ .hP3, and it has a higher energy about 5 kJ/mol of atoms than the stable  $\text{Al}_2\text{RE}$ .cF24 phase in each system. That means that  $\text{Al}_2\text{RE}$ .hP3 can only be a high-temperature phase, perhaps stabilized by a vacancy or substitution mechanism, but such possibility is small based on this paper. Buschow<sup>40</sup> reported that the  $\text{Al}_5\text{La}_2$ .hP3 is stable over a very narrow temperature range 1090–1240 °C, but its exact composition (or more precisely, the composition range) remains unknown to date.<sup>20,21</sup> In contrast to the lanthanide RE elements,  $\text{Al}_2\text{RE}$ .hP3 is stable among the early actinides such as Al-Th (Refs. 20 and 21) and Ac-Al.<sup>32</sup>

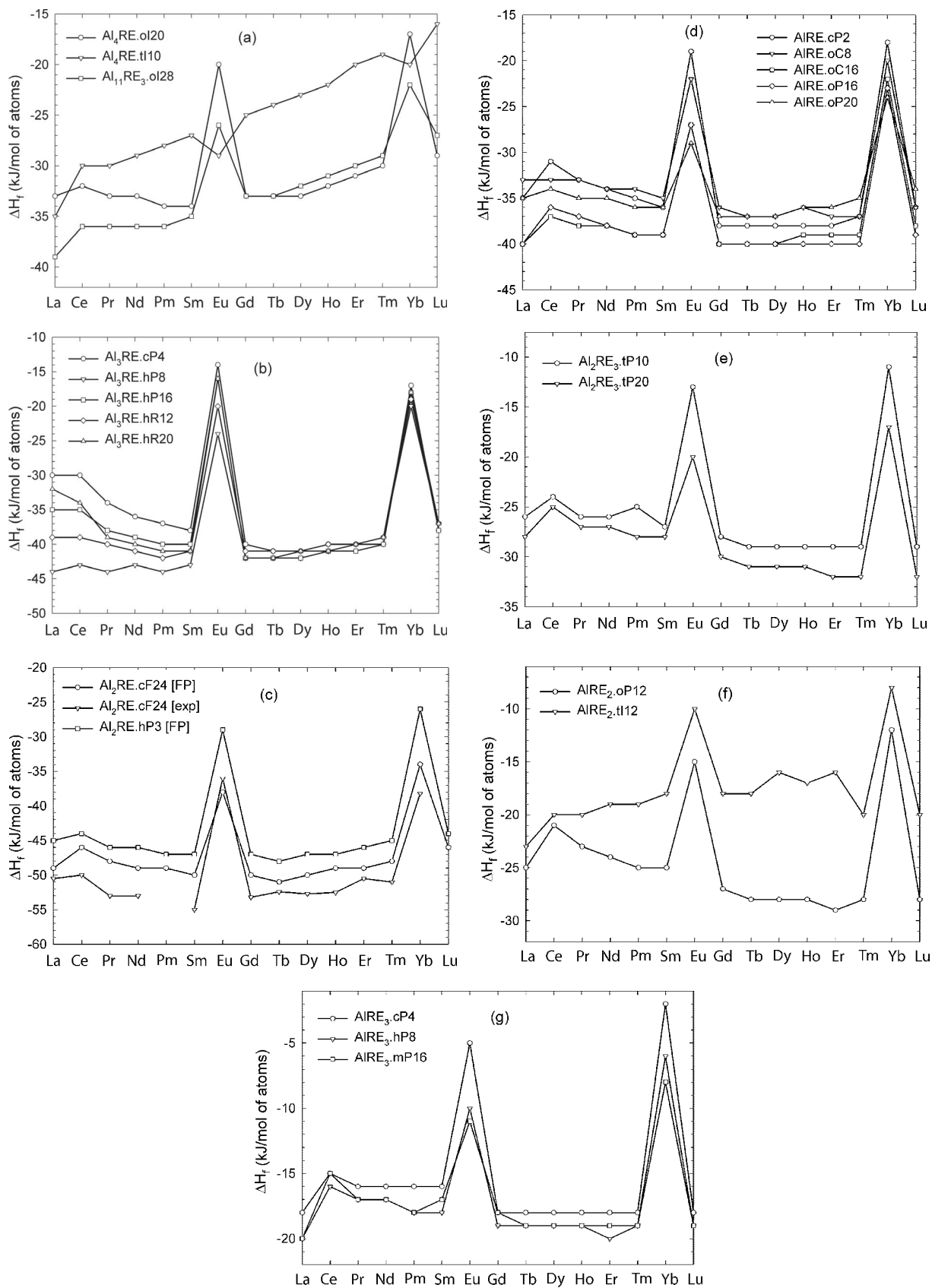


FIG. 4. The trend of the enthalpies of formation of several groups of competing compounds across the Periodic Table: (a)  $Al_4RE$  family, (b)  $Al_3RE$  family, (c)  $Al_2RE$  family, (d) AIRE family, (e)  $Al_2RE_3$  family, (f)  $AIRE_2$  family, and (g)  $AIRE_3$  family. The volume per atom plot is shown in (h) for certain selected compounds.

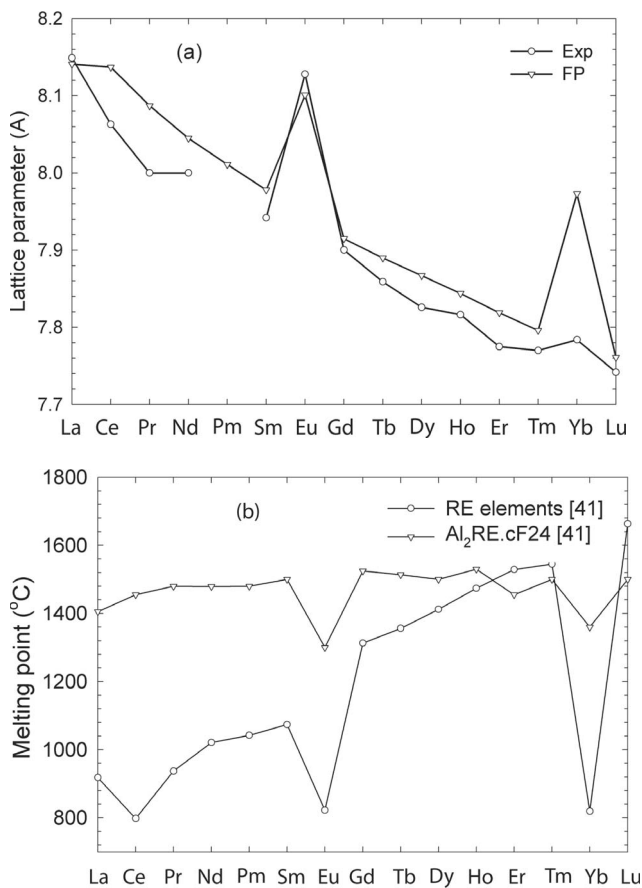


FIG. 5. (a) Comparison of the lattice parameter of  $\text{Al}_2\text{RE} \cdot \text{cF}24$  between experiments and the present FP calculations. (b) The melting point of RE and  $\text{Al}_2\text{RE} \cdot \text{cF}24$ .

#### D. AIRE family (cP2, oC8, oC16, oP16, and oP20) [Figure 4(d)]

Among the equiatomic AIRE compounds, namely,  $\text{Al-RE} \cdot \text{cP}2$ ,  $\text{AlRE} \cdot \text{oC}8$ ,  $\text{AlRE} \cdot \text{oC}16$ ,  $\text{AlRE} \cdot \text{oP}16$ , and  $\text{Al-RE} \cdot \text{oP}20$ , the most likely stable phases are  $\text{AlRE} \cdot \text{oC}16$  and  $\text{AlRE} \cdot \text{oP}16$ , which both have a much lower energy than the others (except for  $\text{RE}=\text{Eu}$ ,  $\text{Yb}$ ). The trend is that  $\text{AlRE} \cdot \text{oP}16$  becomes more stable with increasing RE atomic number, in agreement with experiment. On the other hand,  $\text{AlRE} \cdot \text{oP}20$  is especially favored for divalent Eu and Yb; it has the lowest energy in this family for both elements and  $\text{AlEu} \cdot \text{oP}20$  lies on the convex hull but  $\text{AlYb} \cdot \text{oP}20$  lies above the convex hull by 1.3 kJ.

#### E. $\text{Al}_2\text{RE}_3$ family (tP10 and tP20) [Figure 4(e)]

For the  $\text{Al}_2\text{RE}_3$  compounds, two crystal structures are reported in the Al-RE and Al-An (An=actinides), namely,  $\text{Al}_2\text{Th}_3 \cdot \text{tP}10$  (prototype  $\text{Si}_2\text{U}_3$ ) and  $\text{Al}_2\text{RE}_3 \cdot \text{tP}20$  ( $\text{RE}=\text{Gd}$ ,  $\text{Ho}$ ,  $\text{Tb}$ ,  $\text{Er}$ ,  $\text{Lu}$ ,  $\text{Tm}$ , prototype  $\text{Al}_2\text{Gd}_3$ ). Except Eu and Yb, the overall trend is that both lattices steadily gain stability. However, in all cases,  $\text{Al}_2\text{R}_3 \cdot \text{tP}20$  is more stable than  $\text{Al}_2\text{R}_3 \cdot \text{tP}10$ , as observed in experiments. That is,  $\text{Al}_2\text{RE}_3 \cdot \text{tP}20$  is stable for all late REs including Gd except Yb, and it is not stable for all the early REs.<sup>20,21</sup>

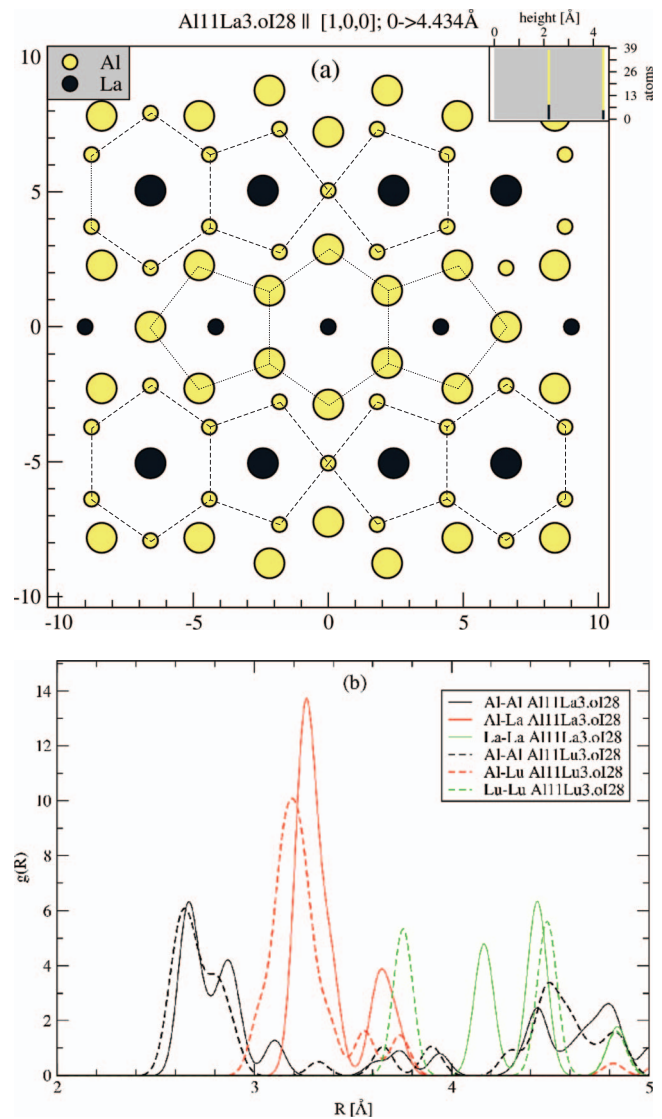


FIG. 6. (Color online) (a) The atomic structure of  $\text{Al}_{11}\text{La}_3 \cdot \text{oI}28$ . The viewing direction is indicated on top of each figure together with the height of repeating unit cell along that direction. The size of atoms indicates their height in the structure along the viewing direction. The caption is the same for Figs. 6–10. (b) Comparison in the pair distribution of  $\text{Al}_{11}\text{La}_3 \cdot \text{oI}28$  vs  $\text{Al}_{11}\text{Lu}_3 \cdot \text{oI}28$ .

#### F. $\text{AlRE}_2$ family (oP12 and tI12) [Figure 4(f)] and $\text{AlRE}_3$ family [Figure 4(g)]

For the  $\text{AlRE}_2$ -type compound, we compare  $\text{AlRE}_2 \cdot \text{oP}12$  with  $\text{AlTh}_2 \cdot \text{tI}12$ . For the complete RE series, oP12 is much more stable than tI12, as observed in experiments. In addition, oP12 is more favored for late REs. Experimentally,  $\text{Al-RE} \cdot \text{oP}12$  does not occur for  $\text{RE}=\text{La}$ , it is only high-temperature (HT) stable for  $\text{RE}=\text{Ce}$ , and then remains stable for all other REs except the divalent  $\text{RE}=\text{Eu}$ ,  $\text{Yb}$ , the untested Pm, and the case of  $\text{RE}=\text{Tm}$  where we predict that it *should* occur.

#### G. $\text{AlRE}_3$ family [Figure 4(g)]

The last class of compounds examined in this study includes the  $\text{AlRE}_3 \cdot \text{cP}4$  (prototype  $\text{AuCu}_3$ ),  $\text{AlRE}_3 \cdot \text{hP}8$  (pro-

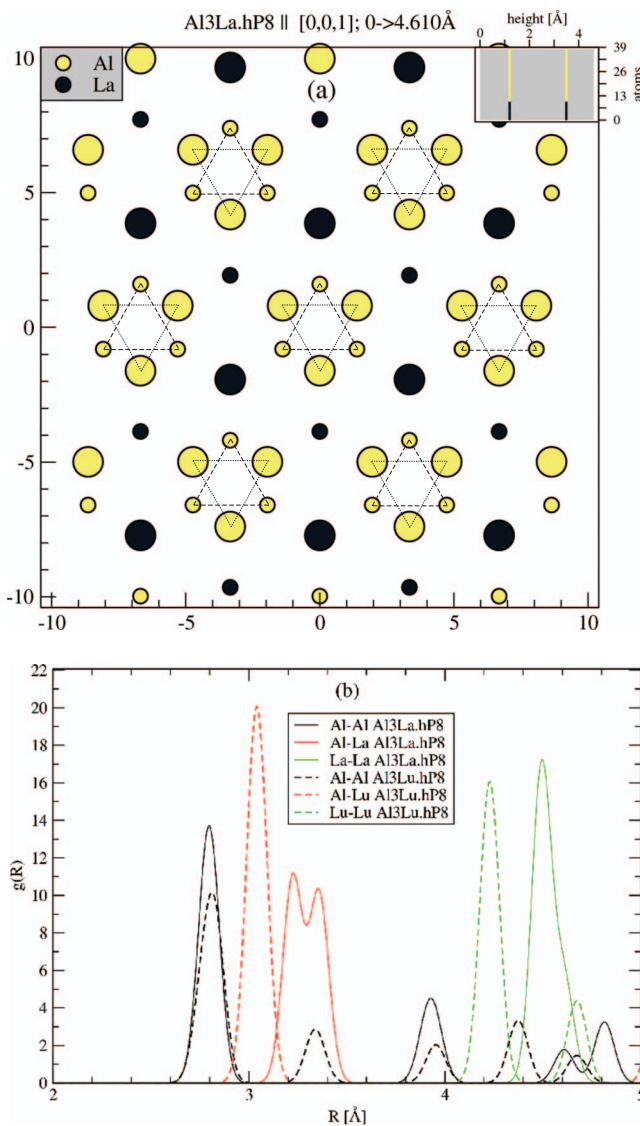


FIG. 7. (Color online) (a) The atomic structure of  $\text{Al}_3\text{La.hP8}$ . (b) Comparison in the pair distribution of  $\text{Al}_3\text{La.hP8}$  vs  $\text{Al}_3\text{Lu.hP8}$ .

totype  $\text{Ni}_3\text{Sn}$ ), and  $\text{AIRE}_3.\text{mP16}$  (prototype  $\text{AlCe}_3$ ). Our calculations predict that in all cases, the  $\text{AIRE}_3.\text{hP8}$  has a lower energy than the  $\text{AIRE}_3.\text{cP4}$ . The experiments showed that the  $\text{AIRE}_3.\text{hP8}$  is the low-temperature allotrope and  $\text{AIRE}_3.\text{cP4}$  the allotrope at high temperatures<sup>20,21</sup> for Ce and Pr, the two cases where hP8 is stable. Again, exception occurs at Eu and Yb for both families.

## V. DISCUSSION

We now re-examine some of the notable trends in structural stability across the entire Al-RE series. As previously noted, alloys of the divalent RE elements Eu and Yb will usually be exceptions to the trends, which hold mainly for the remaining (trivalent) RE elements. Also, Ce is often a special case as well. The trends we seek to explain are that (1)  $\text{Al}_{11}\text{RE}_3.\text{oI28}$  is stable only for the early RE elements and loses stability to  $\text{Al}_3\text{RE.hP8}$  for late REs; (2)  $\text{Al}_2\text{RE.cF24}$  is stable across the entire RE series, consis-

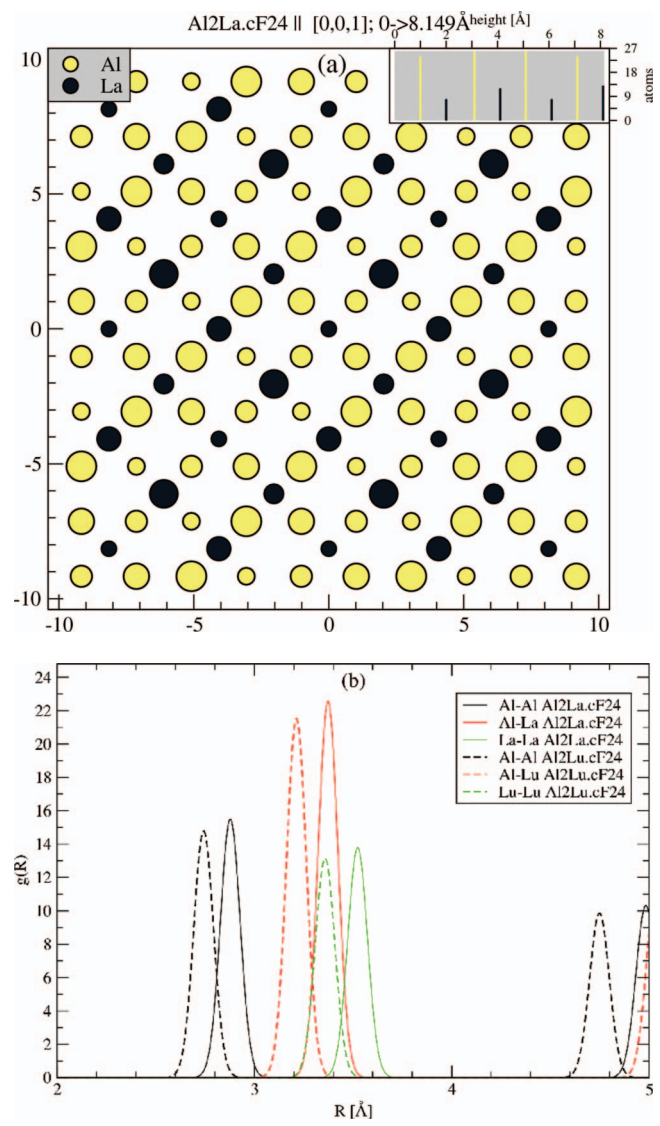


FIG. 8. (Color online) (a) The atomic structure of  $\text{Al}_2\text{La.cF24}$ . (b) Comparison in the pair distribution of  $\text{Al}_2\text{La.cF24}$  vs  $\text{Al}_2\text{Lu.cF24}$ .

tently beating  $\text{Al}_2\text{RE.hP3}$  which, however, is stable for some actinide RE elements; (3) for early REs,  $\text{Al}_3\text{RE.hP8}$  is much more stable than other  $\text{Al}_3\text{RE}$  structures, but for later REs, there is near degeneracy among hP8, cP4, hP16, hR12, and hR20 and hence a likelihood of allotropes; and (4) the equiatomic AIRE structures oP16 and oC16 are nearly degenerate for early REs, while oP16 is distinctly favored for late REs.

Our analysis relies on the trend of reduction in atomic size across the RE series. We focus on RE=La and Lu as the extreme ends of the RE series (since the atomic size of other REs falls between them except at Ce, Eu, and Yb) and also as cases where the potentials seem very satisfactory. To estimate atomic sizes, we examined the near-neighbor peaks of the pair correlation function  $g(r)$ . We take 2.8 Å as the ideal Al-Al separation, 3.7 Å as ideal for La-La, and 3.4 Å for Lu-Lu. Pair potentials for pure Al (Ref. 54) exhibit a soft shoulder in the range 2.7–2.9 Å. We shall also require the

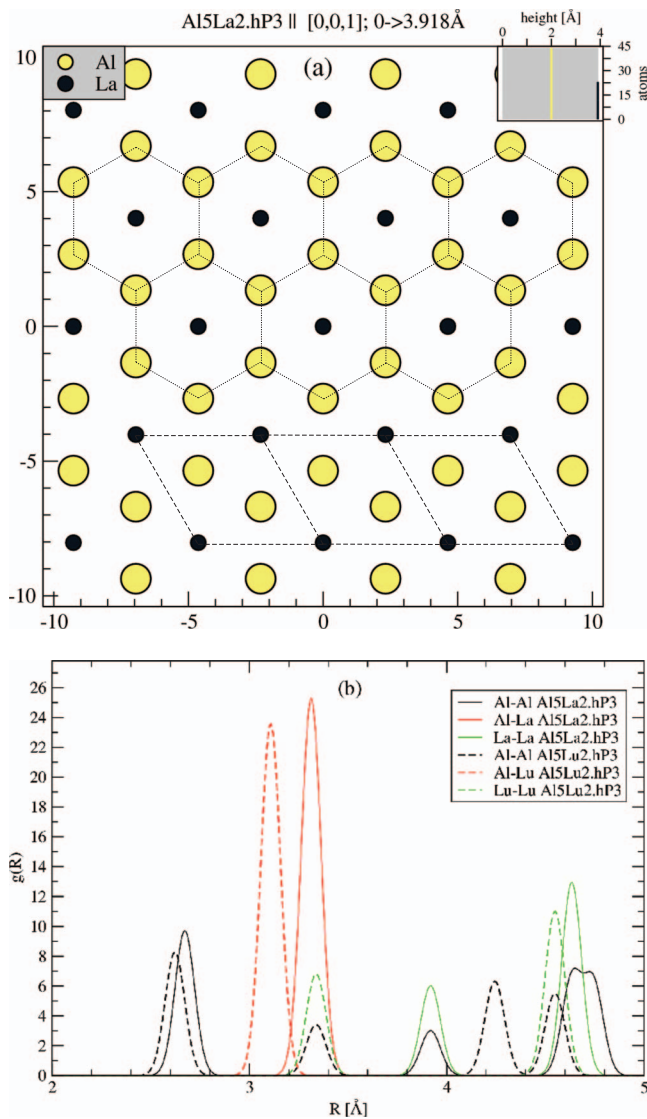


FIG. 9. (Color online) (a) The atomic structure of  $\text{Al}_2\text{La.hP3}$ . (b) Comparison in the pair distribution of  $\text{Al}_2\text{La.hP3}$  vs  $\text{Al}_2\text{Lu.hP3}$ .

ideal Al-RE separations, which we take as 3.25 Å for Al-La and 3.0 Å for Al-Lu based on the  $\text{Al}_3\text{RE.hP8}$  structures.

To explain the loss of  $\text{Al}_{11}\text{RE}_3.\text{oI28}$  stability to  $\text{Al}_3\text{RE.hP8}$  (in coexistence with pure elemental Al) from early to late REs, we examine the atomic structure and pair correlations shown in Fig. 6. Evidently,  $\text{oI28}$  consists of isolated RE atoms at the centers of pentagonal and hexagonal prisms. The in-plane Al-Al separation is governed by the Al-RE bond length. For the large La atom, the Al-Al distance is a short 2.62 Å while the Al-La distance is close to the optimal 3.25 Å. When the prisms are centered by the smaller Lu atom, the Al-Lu bond is squashed to a short 3.15 Å, while the Al-Al bond is even slightly further compressed to provide a balance of forces. Consequently, the enthalpy of  $\text{oI28}$  increases by +10 kJ/mol across the RE series. This effect is reflected in the density of states (not shown), which exhibits a pseudogap at the Fermi surface for Al-La but not for Al-Lu. A pseudogap is often associated with satisfying interatomic bond lengths.

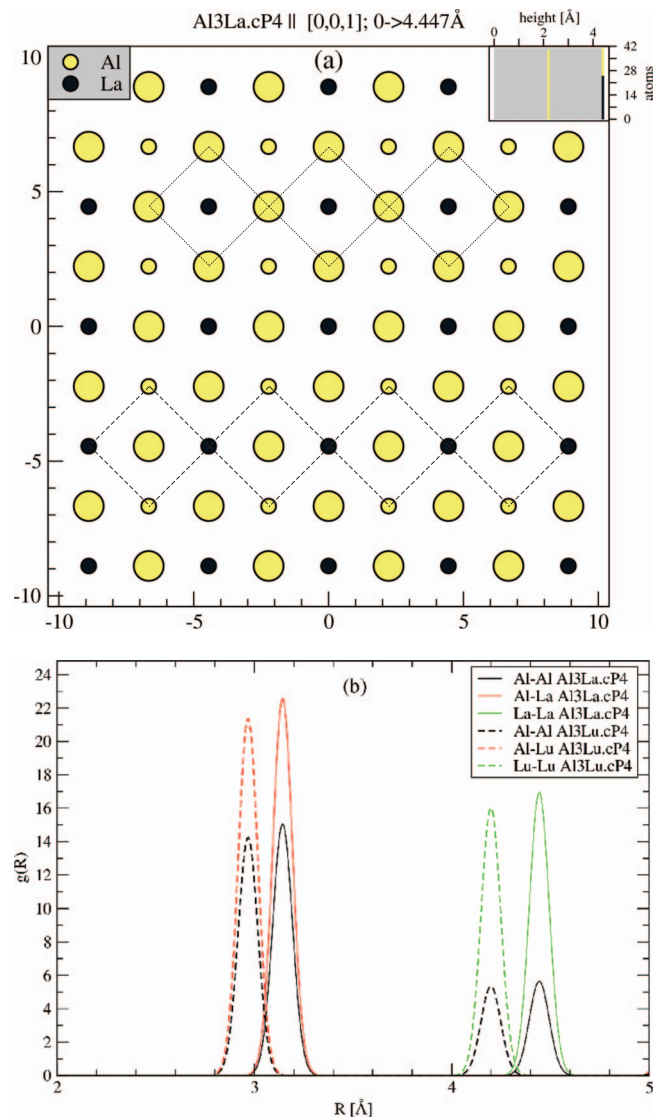


FIG. 10. (Color online) (a) The atomic structure of  $\text{Al}_3\text{La.cP4}$ . (b) Comparison in the pair distribution of  $\text{Al}_3\text{La.cP4}$  vs  $\text{Al}_3\text{Lu.cP4}$ .

Meanwhile, the  $\text{hP8}$  structure (Fig. 7) consists of  $\text{Al}_6$  octahedra straddling the planes of a hexagonal-close-packed lattice of RE atoms. As the RE atom size varies, the lattice can expand or contract to accommodate the change in size with little change in the Al-Al bond length. The enthalpy of  $\text{hP8}$  grows by only 5 kJ/mol across the RE series. Combined with the larger increase in enthalpy of  $\text{oI28}$ , the result is to destabilize  $\text{Al}_{11}\text{RE}_3.\text{oI28}$  in favor of  $\text{Al}_3\text{RE.hP8}$  for late REs.

Next, we compare  $\text{Al}_2\text{RE.cF24}$  with  $\text{Al}_2\text{RE.hP3}$ . The relevant structures are illustrated in Fig. 8. In these highly symmetric structures, all atomic sites sit at special Wyckoff sites with fixed rational coordinates. The only adjustable parameters in these structures are the lattice parameters.  $\text{cF24}$  being cubic has only a single adjustable parameter. Inspecting Fig. 8, it is evident that the lattice parameter adjusts to compromise slightly long Al-RE bonds with slightly short RE-RE bonds and reasonable Al-Al bonds.

In the case of  $\text{hP3}$ , the two independent parameters are  $a$  and  $c$ . Band-structure calculations (not shown) suggest that

the  $c$  axis is governed by pseudogap at the “A” point  $(0,0,\pi/c)$ . Notice (Fig. 9) that in both cases, the Al-Al bond is very short and the Al-RE bond slightly too long. Clearly, there is no satisfactory choice of the  $a$ -axis parameter, because reducing  $a$  to shorten the Al-RE bond will result in further compressing the Al-Al bond, while increasing  $a$  to lengthen the Al-Al bond will further stretch the Al-RE bond.

The third observation is the large spread in enthalpy among the  $\text{Al}_3\text{RE}$  family for early REs but the near degeneracy for late REs [see Fig. 4(b)]. We have already discussed the favorability of hP8 and its tolerance to substitution among RE elements. Why are the other  $\text{Al}_3\text{RE}$  so strongly disfavored for early REs? The effect is most pronounced in the case of cP4, so our discussion concentrates on this case. Since all atoms occupy high-symmetry positions, the only adjustable parameter is the cubic lattice constant. Owing to the geometrical equivalence of the Al and RE sites, the Al-Al separation and the Al-RE separation match identically (see Fig. 10). Thus, the cP4 structure cannot tolerate a large size disparity between species, strongly disfavoring the early RE compounds.

## VI. CONCLUSIONS

Using FP-DFT calculations on over 350 compounds in 15 Al-RE (RE=rare earth elements) binary systems, we conclude the following:

(1) The phase stabilities at 0 K obtained by the FP-DFT calculations agree with experiment for the majority of systems.

(2) The impact of choice of standard or trivalent and/or divalent potentials is examined together with the role of magnetization due to spin-orbital coupling.

(3) Several observed trends in the Al-trivalent RE phase diagrams are explained by the atomic structures of the lattices.

(4) Anomalies occur at Eu and Yb caused by their unique electronic structures.

(5) A possibility of allotropes of the  $\text{Al}_3\text{RE}$  family is suggested based on current calculations, which deserve attention of future experimental studies.

(6) It is confirmed that the AlEu.oP20 is stable in Al-Eu rather than the AlEu.oP18 suggested in Refs. 20 and 21.

## ACKNOWLEDGMENTS

M.C.G. and A.D.R. acknowledge financial support from the Computational Materials Science Network, a program of the Office of Science, US Department of Energy, and from MRSEC through Grant No. DMR-0520425. M.W. acknowledges partial support from NSF through Grant No. DMR-0111198. M.C.G. is grateful for encouragement on this work from Gregory S. Rohrer. We thank Marek Mihalkovic for software development which aided the current research.

\*Corresponding author FAX: +1-412-268-7596. Electronic address: cg2r@alumni.virginia.edu

<sup>1</sup>D. de Fontaine and C. Wolverton, *Ber. Bunsenges. Phys. Chem.* **96**, 1503 (1992).

<sup>2</sup>M. Asta, R. McCormack, and D. de Fontaine, *Phys. Rev. B* **48**, 748 (1993).

<sup>3</sup>G. Rubin and A. Finel, *J. Phys.: Condens. Matter* **7**, 3139 (1995).

<sup>4</sup>V. Ozolins, C. Wolverton, and A. Zunger, *Phys. Rev. B* **57**, 6427 (1998).

<sup>5</sup>I. Al-Lehyani, M. Widom, Y. Wang, N. Moghadom, G. M. Stocks, and J. A. Moriarty, *Phys. Rev. B* **64**, 075109 (2001).

<sup>6</sup>C. Woodward, M. Asta, G. Kresse, and J. Hafner, *Phys. Rev. B* **63**, 094103 (2001).

<sup>7</sup>C. Wolverton and V. Ozolins, *Phys. Rev. Lett.* **86**, 5518 (2001).

<sup>8</sup>A. van de Walle, M. Asta, and G. Ceder, *CALPHAD: Comput. Coupling Phase Diagrams Thermochem.* **26**, 539 (2002).

<sup>9</sup>Y. Wang *et al.*, *CALPHAD: Comput. Coupling Phase Diagrams Thermochem.* **28**, 79 (2004).

<sup>10</sup>M. Mihalkovic and M. Widom, *Phys. Rev. B* **70**, 144107 (2004).

<sup>11</sup>S. Curtarolo, D. Morgan, and G. Ceder, *CALPHAD: Comput. Coupling Phase Diagrams Thermochem.* **29**, 163 (2005).

<sup>12</sup>M. C. Gao *et al.*, *Metall. Mater. Trans. A* **36A**, 3269 (2005).

<sup>13</sup>G. Ghosh and M. Asta, *Acta Mater.* **53**, 3225 (2005).

<sup>14</sup>K. Ozturk *et al.*, *Metall. Mater. Trans. A* **36A**, 5 (2005).

<sup>15</sup>R. Arroyave, A. van de Walle, and Z. K. Liu, *Acta Mater.* **54**, 473 (2006).

<sup>16</sup>M. H. F. Sluiter, *CALPHAD: Comput. Coupling Phase Diagrams Thermochem.* **30**, 357 (2006).

<sup>17</sup>C. Wolverton and V. Ozolins, *Phys. Rev. B* **73**, 144104 (2006).

<sup>18</sup>M. C. Gao, A. D. Rollett, and M. Widom, *CALPHAD: Comput. Coupling Phase Diagrams Thermochem.* **30**, 341 (2006).

<sup>19</sup>G. Zanicchi *et al.*, *Intermetallics* **12**, 363 (2004).

<sup>20</sup>T. B. Massalski *et al.*, *Binary Alloy Phase Diagrams* (ASM International, Materials Park, OH, 1995).

<sup>21</sup>H. Okamoto, *Desk Handbook: Phase Diagrams for Binary Alloys* (ASM International, Materials Park, OH, 2000).

<sup>22</sup>K. A. Gschneidner, *J. Less-Common Met.* **17**, 1 (1969).

<sup>23</sup>K. A. Gschneidner, *J. Less-Common Met.* **25**, 405 (1971).

<sup>24</sup>P. Strange *et al.*, *Nature (London)* **399**, 756 (1999).

<sup>25</sup>A. Delin, L. Fast, B. Johansson, J. M. Wills, and O. Eriksson, *Phys. Rev. Lett.* **79**, 4637 (1997).

<sup>26</sup>B. Johansson, *Phys. Rev. B* **20**, 1315 (1979).

<sup>27</sup>K. A. Gschneidner and R. M. Valletta, *Acta Metall.* **16**, 477 (1968).

<sup>28</sup>K. A. Gschneidner and W. B. Pearson, *Mater. Res. Bull.* **3**, 951 (1968).

<sup>29</sup>G. Kresse and J. Hafner, *Phys. Rev. B* **47**, 558 (1993).

<sup>30</sup>G. Kresse and J. Furthmuller, *Phys. Rev. B* **54**, 11169 (1996).

<sup>31</sup>J. P. Perdew, K. Burke, and M. Ernzerhof, *Phys. Rev. Lett.* **77**, 3865 (1996).

<sup>32</sup>M. C. Gao, A. D. Rollett, and M. Widom, TMS Annual Meeting 2007: Proceedings of the Symposium on Computational Thermodynamics and Phase Transformations, Orlando, FL, 2007, (unpublished).

<sup>33</sup>P. Villars, *Pearson's Handbook*, desk ed. (ASM International, Materials Park, OH, 1997).

- <sup>34</sup>P. J. Craievich, M. Weinert, J. M. Sanchez, and R. E. Watson, *Phys. Rev. Lett.* **72**, 3076 (1994).
- <sup>35</sup>P. J. Craievich, J. M. Sanchez, R. E. Watson, and M. Weinert, *Phys. Rev. B* **55**, 787 (1997).
- <sup>36</sup>L. G. Wang, M. Sob, and Z. Y. Zhang, *J. Phys. Chem. Solids* **64**, 863 (2003).
- <sup>37</sup>Y. Wang, R. Ahuja, M. C. Qian *et al.*, *J. Phys.: Condens. Matter* **14**, L695 (2002).
- <sup>38</sup>J. Z. Liu, A. van de Walle, G. Ghosh, and M. Asta, *Phys. Rev. B* **72**, 144109 (2005).
- <sup>39</sup>S. H. Zhou and R. E. Napolitano, *Acta Mater.* **54**, 831 (2006).
- <sup>40</sup>K. H. J. Buschow, *Philips Res. Rep.* **20**, 337 (1965).
- <sup>41</sup>K. H. J. Buschow and J. H. Vanvucht, *Philips Res. Rep.* **22**, 233 (1967).
- <sup>42</sup>K. A. J. Gschneidner and F. W. Calderwood, *Bull. Alloy Phase Diagrams* **9**, 658 (1988).
- <sup>43</sup>K. A. Gschneidner, *Acta Crystallogr.* **18**, 1082 (1965).
- <sup>44</sup>K. A. J. Gschneidner, *J. Alloys Compd.* **193**, 1 (1993).
- <sup>45</sup>G. Borzone, G. Cacciamani, and R. Ferro, *Metall. Trans. A* **22**, 2119 (1991).
- <sup>46</sup>G. Borzone *et al.*, *Z. Metallkd.* **84**, 635 (1993).
- <sup>47</sup>A. Saccone *et al.*, *Intermetallics* **6**, 201 (1998).
- <sup>48</sup>G. Borzone *et al.*, *J. Alloys Compd.* **220**, 122 (1995).
- <sup>49</sup>G. Borzone *et al.*, *Intermetallics* **11**, 1217 (2003).
- <sup>50</sup>G. Borzone, R. Raggio, and R. Ferro, *Phys. Chem. Chem. Phys.* **1**, 1487 (1999).
- <sup>51</sup>F. Sommer and M. Keita, *J. Less-Common Met.* **136**, 95 (1987).
- <sup>52</sup>F. Sommer, M. Keita, H. G. Krull *et al.*, *J. Less-Common Met.* **137**, 267 (1988).
- <sup>53</sup>C. Colinet, A. Pasturel, and K. H. J. Buschow, *J. Chem. Thermodyn.* **17**, 1133 (1985).
- <sup>54</sup>J. A. Moriarty and M. Widom, *Phys. Rev. B* **56**, 7905 (1997).
- <sup>55</sup>S. Meschel and O. Kleppa, *J. Alloys Compd.* **197**, 75 (1993).
- <sup>56</sup>V. Kober *et al.*, *Izv. Vyssh. Uchebn. Zaved., Tsvetn. Metall.* **5**, 83 (1977).
- <sup>57</sup>V. Kober *et al.*, *Izv. Vyssh. Uchebn. Zaved., Tsvetn. Metall.* **3**, 58 (1983).
- <sup>58</sup>R. Ferro *et al.*, *J. Phase Equilib.* **15**, 317 (1994).
- <sup>59</sup>A. Pastural *J. Less-Common Met.* **90**, 21 (1983).
- <sup>60</sup>V. Kober *et al.*, *Izv. Vyssh. Uchebn. Zaved., Tsvetn. Metall.* **5**, 101 (1982).
- <sup>61</sup>V. Kober *et al.*, *Izv. Vyssh. Uchebn. Zaved., Tsvetn. Metall.* **22**, 144 (1979).
- <sup>62</sup>C. Colinet, A. Pasturel, and K. H. J. Buschow, *Physica B & C* **150**, 397 (1988).
- <sup>63</sup>W. G. Jung, O. J. Kleppa, and L. Topor, *J. Alloys Compd.* **176**, 309 (1991).